Journal of Catalysis **185,** 423–434 (1999)
Article ID jcat.1999.2516, available online at http://www.idealibrary.com on IDEAL®

FTIR Study of Adsorption and Reactions of Methyl Formate on Powdered TiO_2

Chih-Chung Chuang, Wen-Chun Wu, Ming-Chih Huang, I-Chieh Huang, and Jong-Liang Lin[1]

Department of Chemistry, National Cheng Kung University, Tainan, Taiwan, Republic of China

Received December 15, 1998; revised April 3, 1999; accepted April 5, 1999

Adsorption, thermochemistry, and photochemistry of methyl formate on powdered TiO_2 have been studied by Fourier-transformed infrared spectroscopy. Methyl formate is adsorbed on the TiO_2 surface in two forms. One is molecularly adsorbed methyl formate showing a red-shifted carbonyl stretching. The other is a structure-reorganized species showing absorption bands at 2841, 2866, and 2942 cm^{-1} in the CH_x stretching region. An orthoester-type intermediate is proposed to explain the observed infrared absorption bands. In the thermal reactions, all the detected carbon-containing gas products are derived from $CH_3O_{(a)}$ and $HCOO_{(a)}$, which are generated as surface intermediates in the process of methyl formate decomposition. In methyl formate photochemistry, both O_2 and TiO_2 are essential. The origins of the gas products relating to the adsorbed species are also discussed.

Key Words: **FTIR; methyl formate; TiO_2; adsorption; photochemistry.**

INTRODUCTION

Methyl formate (MF) has been generated by processes including direct carbonylation of methanol, dehydrogenative coupling of two methanol molecules, Tischenko dimerization of formaldehyde, direct synthesis from synthesis gas, esterification of formic acid with methanol, and oxidative dehydrogenation of methanol (1). A chemical process (as shown in Scheme 1) for oxidative dehydrogenation of methanol to MF on an oxygen preadsorbed Ag(110) surface has been proposed (2). In this reaction pathway, methanol is dissociatively adsorbed to form methoxy groups ($CH_3O_{(a)}$), which may in turn decompose to form adsorbed CH_2O on the surface. The adsorbed CH_2O then reacts with the $CH_3O_{(a)}$ to form hemiacetal alcoholate intermediate that subsequently undergoes the rate-limiting decomposition to generate MF. On the other hand, MF has been used as a versatile chemical intermediate in a variety of reactions, such as hydrogenolysis to form methanol, homologation to elongate the carbon-chain length, and carbonyl transfer to amines to form amides (1). Surface vibrational studies of adsorbed MF and/or its thermal reactions on metals (2–5), metal oxides (6–8), and supported metal catalysts (9–13) have been reported. It has been proposed that, on an oxygen preadsorbed Ag(110) surface, MF is adsorbed via the carbonyl oxygen coupling to a surface Ag atom, followed by a nucleophilic attack at the carbonyl carbon from surface oxygen ion, forming a tetrahedral orthoester-type species that subsequently decomposes to yield $CH_3O_{(a)}$ and formate species ($HCOO_{(a)}$) (14). Scheme 2 shows the surface reaction process. It is interesting to note that the decomposition process of MF as shown in this scheme does not follow the reverse route for the formation of MF in Scheme 1. A similar reaction pathway for the formation of MF from adsorbed CH_2O and $CH_3O_{(a)}$ on copper-based catalysts via hemiacetal intermediate has also been proposed (13, 15–17). However, in decomposition of MF on these catalysts, hemiacetal species is thought to be the reaction intermediate (18).

In the past few decades, thermal reactions and photochemistry of organic compounds on TiO_2 have been widely studied due to their potential for conversion of environmental pollutants into innocuous products and for making industrial materials (19, 20). In the previous study of photooxidative degradation of methanol over TiO_2 in the presence of oxygen, MF was generated as a partial oxidation product (21, 22). However, detailed study of MF interacting with TiO_2 has not been reported. In this paper, we study adsorption and reactions of MF on TiO_2 by Fourier-transformed infrared spectroscopy (FTIR). To identify the species on the TiO_2 after MF adsorption followed by annealing under vacuum, formic acid (precursor for formate groups), methanol (precursor for methoxy groups), $CH_3OCH_2OCH_3$ (dimethoxymethane, DMM, possible precursor for hemiacetal species), and ICH_2OCH_3 (iodomethyl methyl ether, IMME, another possible precursor for hemiacetal species) are investigated as well.

[1] To whom correspondence should be addressed at Department of Chemistry, National Cheng Kung University, 1, Ta Hsueh Road, Tainan, Taiwan, Republic of China. E-mail: jonglin@mail.ncku.edu.tw. Fax: 011-886-6-2740552.

0021-9517/99 $30.00

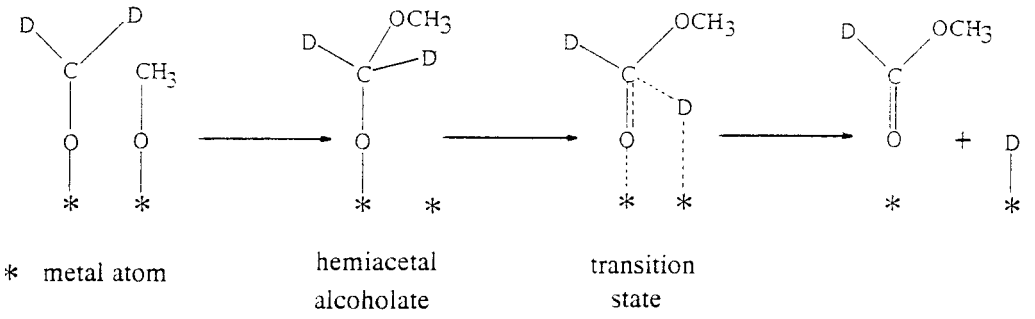

SCHEME 1

EXPERIMENTAL

The experiments were carried out in a high-temperature stainless-steel infrared cell with two CaF_2 windows for IR transmission down to 1000 cm^{-1} and a quartz window for UV transmission (23). The IR cell was connected to a gas manifold that was pumped by a 60 liter/s turbomolecular pump with a base pressure of $\sim 1 \times 10^{-7}$ Torr. The powdered TiO_2 used in the study was supported on a tungsten grid of ~ 6 cm^2. This grid was held in a pair of stainless-steel clamps that were attached to the power leads of a power/thermocouple feedthrough. Temperature of the TiO_2 was measured by a K-type thermocouple spot-welded on the tungsten grid, raised by resistive heating, and controlled by a temperature programmer. The TiO_2 supported on the tungsten grid was prepared according to the procedure reported previously (24). In brief, TiO_2 powder (Degussa P 25, ~ 50 m^2/g; anatase, $\sim 70\%$; rutile, $\sim 30\%$) (25) was well dispersed in water/acetone solution to form a uniform mixture that was then sprayed onto the entire area of the tungsten grid. The TiO_2 sample was subsequently mounted in the IR cell and positioned with its normal direction $\sim 45°$ to both the IR and UV beams for simultaneous photochemistry and FTIR. The sample in the IR cell was then outgassed at 480°C under vacuum for 24 h to remove adsorbed hydrocarbons. Before each run of the experiment, the TiO_2 sample was outgassed at 480°C for 2 h under vacuum and cooled back down to ~ 35°C for gas exposure. Oxygen (99.998%, Matheson), MF (99%, Aldrich), formic acid (>98%, Merck), methanol (99.8%, BDH), IMME (95%, Aldrich), and DMM (98%, TCI) were used in this research. All of the liquid compounds were further purified by several cycles of freeze–pump–thaw. Pressure of the system was monitored by a Baratron capacitance manometer and an ion gauge. The UV light source used was a 350-W Hg arc lamp (Oriel Corp.) with a water filter in front of the photon exit. The power, measured in the air by a power meter, at the position of the TiO_2 sample was ~ 0.9 W/cm^2. Infrared spectra were obtained with 4 cm^{-1} resolution using a Bruker FTIR spectrometer with a MCT detector. The entire IR optical path was purged with CO_2-free dry air. The infrared spectra presented in this paper have been ratioed against a clean TiO_2 spectrum.

RESULTS

Adsorption of formic acid. Figure 1 shows the IR spectra after formic acid adsorption on TiO_2 followed by evacuation at the indicated temperatures. For the TiO_2 sample at 35°C, absorption bands at 1275, 1324, 1371, 1552, 1675, 1725, 2737, 2871, and 2952 cm^{-1} are observed in the spectrum. After heating the sample under vacuum to 150°C, the most obvious change in the spectrum is that the bands at 1675 and 1725 cm^{-1} become barely visible and a small new band is revealed at 1670 cm^{-1}. The band at ~ 1278 cm^{-1} becomes more resolved. Besides, two narrow bands appear at 1386 and 1413 cm^{-1}. The other bands show their positions at 1332, 1359, 1370, 1537, 1552, 2754, 2872, 2952,

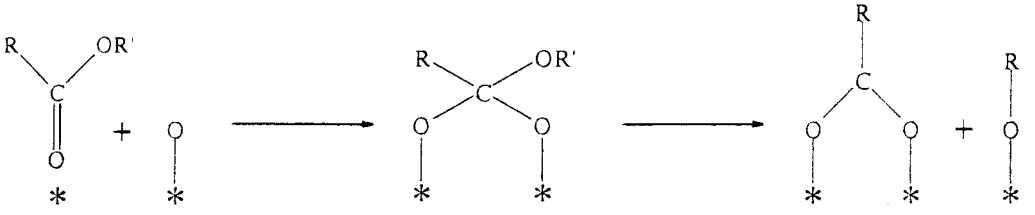

SCHEME 2

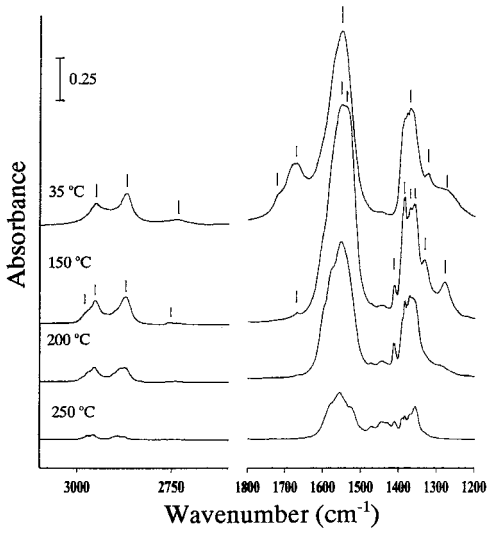

FIG. 1. Infrared spectra of the TiO_2 at 35°C after being in contact with 2 Torr of formic acid followed by evacuation at the indicated temperatures for 1 min. All the spectra were obtained with 50 scans. The TiO_2 powder used was 0.085 g. The absorption frequencies at the marked positions are listed in the text.

and 2977 cm^{-1}. The disappearance of the bands at 1675 and 1725 cm^{-1}, assignable to carbonyl stretch, can be attributed to the desorption and/or dissociation of adsorbed formic acid molecules. Its carbonyl stretching frequencies are lower than the carbonyl stretching frequency of formic acid in gas phase by ~15–65 cm^{-1}. The bands at 1278, 1332, and 1670 cm^{-1} are probably due to more strongly adsorbed formic molecules. The first two bands may be assigned to the C–O stretching or C–H bending and the third one to the carbonyl stretching (26). The bands at 1359, 1370, 1386, 1413, 1537, 1552, 2754, 2872, 2952, and 2977 cm^{-1}, based on previous reports (27, 28), are due to adsorbed formate species. The bands at 1359 and 1370 cm^{-1} are attributed to $-CO_2-$ symmetric stretch, at 1386 and 1412 cm^{-1} to C–H deformation or $-CO_2-$ rocking (29), at 1537 and 1552 cm^{-1} to $-CO_2-$ antisymmetric stretch, at 2754 cm^{-1} to a combination mode of symmetric $-CO_2-$ stretch and CH deformation, at 2872 cm^{-1} to CH stretch, and at 2952 and 2977 cm^{-1} to a combination of antisymmetric $-CO_2-$ stretch and CH deformation. Furthermore, the frequency differences between the $-CO_2-$ antisymmetric and symmetric stretches are close to those of formate ions or formate salt, indicating that most of the formate groups on the TiO_2 surface are adsorbed with bridging coordination; i.e., the two oxygen atoms of the formate groups are bonded to two different Ti ions on the surface (29). After raising the TiO_2 to higher temperatures, all of the bands are considerably reduced in intensity.

Adsorption of methanol. Figure 2 presents the IR spectra after methanol adsorption on TiO_2 followed by evacuation at the indicated temperatures. Our results are similar to the previous studies of methanol adsorption on TiO_2 (30–32). For the spectrum at 35°C, bands at 2820, 2846, 2890, 2910, 2926, and 2947 cm^{-1} are observed. Two identifiable species are present on the surface. One is adsorbed methanol molecules with the major absorptions at 2846 and 2947 cm^{-1}. The other one is adsorbed methoxy groups with the major bands at ~2820 and ~2926 cm^{-1}. They are assigned to symmetric and antisymmetric $-CH_3-$ stretches, respectively. After raising the surface temperature to 150°C, the surface concentration of methanol is significantly diminished and the surface is dominated with methoxy groups. After increasing the TiO_2 temperature above 250°C, the amount of the methoxy is largely decreased.

Adsorption of methyl formate. Figure 3 presents the IR spectra after MF adsorption on TiO_2 followed by evacuation at the indicated temperatures. For the spectrum at 35°C, the absorption bands at 1263, 1355, 1388, 1412, 1438, 1458, 1545, 1588, 1675, 2757, 2827, 2862, 2895, 2928, 2938, 2960, and 3040 cm^{-1} are observed. The residual surface OH groups on the TiO_2 are reduced in intensity upon MF adsorption as shown in the region of 3500–3800 cm^{-1}. After heating the TiO_2 sample under vacuum to 150°C, the bands at 1263, 1438, 1458, 1675, 2960, and 3040 cm^{-1} almost disappear. Other bands show their positions at 1355, 1388, 1412, 1530, 1584, 2760, 2832, 2866, 2897, and 2943 cm^{-1}. By comparing the absorption frequencies in Fig. 3 with standard infrared absorption ones, previously reported results, and our experimental results in Figs. 1 and 2, the assignment for the bands in Fig. 3 can be made. First of all, the absorption of 1675 cm^{-1} in the spectrum at 35°C in Fig. 3 is within the possible frequency range of carbonyl stretch and is ~80 cm^{-1} less than that of MF in the gas phase (1755 cm^{-1}). This redshifted absorption is very likely due to the adsorbed MF interacting with the TiO_2 surface. The possible reason for

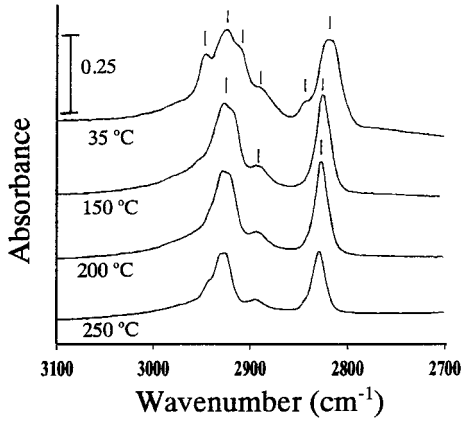

FIG. 2. Infrared spectra of the TiO_2 at 35°C after being in contact with 2 Torr of methanol followed by evacuation at the indicated temperatures for 1 min. All the spectra were obtained with 50 scans. The TiO_2 powder used was 0.085 g. The absorption frequencies at the marked positions are listed in the text.

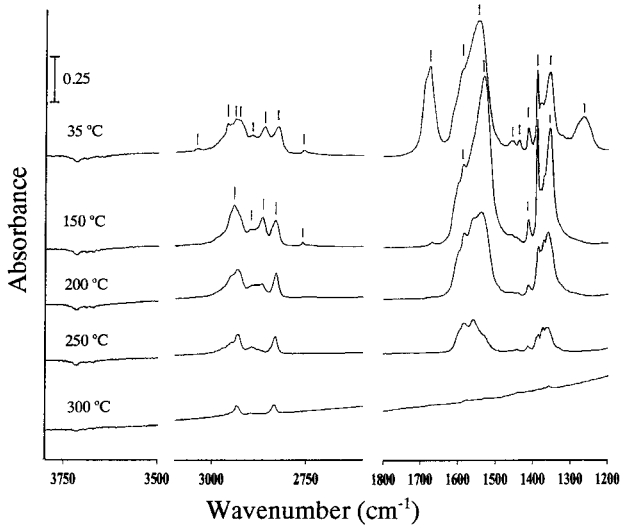

FIG. 3. Infrared spectra of the TiO_2 at 35°C after being in contact with 2 Torr of methyl formate followed by evacuation at the indicated temperatures for 1 min. All the spectra were obtained with 50 scans. The TiO_2 powder used was 0.085 g. The absorption frequencies at the marked positions are listed in the text.

the lower carbonyl absorption frequency and the comparison with previously reported MF adsorption on various surfaces is discussed in the next section. Upon raising the TiO_2 temperature to 150°C, this carbonyl absorption becomes barely visible, accompanying the disappearance of several bands at 1263, 1438, 1458, 2959, and 3040 cm^{-1}. The loss of these bands may result from the MF desorption from and/or reaction with the TiO_2 surface. Second, the bands at 1355, 1388, 1412, 1530, and 1588 cm^{-1} in Fig. 3 are identified as arising from surface formate groups. Third, the bands at ~2830 and ~2930 cm^{-1} in Fig. 3 are assigned to the symmetric and antisymmetric –CH_3– stretch of adsorbed methoxy groups, respectively. Last, under Discussion, the bands of 2862 and 2943 cm^{-1} at 150°C in Fig. 3 are identified. After raising the TiO_2 temperature to 200°C, the surface amount of formate groups is decreased in addition to the decreasing intensities of 2866 and 2943 cm^{-1}. For higher annealing temperatures, all of the surface species are further reduced in concentration.

Thermal reactions of MF over TiO_2. Figure 4 shows the IR results of thermal reactions of 2 Torr of MF over TiO_2. The spectrum at 35°C in Fig. 4 is similar to that of MF in the gas phase. The IR absorption signals from the surface species in Fig. 4 are much smaller than those from the surface species in Fig. 3, because the amount of TiO_2 used is also much less than that used in Fig. 3. Upon linearly heating the TiO_2 at 2°C/s to 290°C, the signals of the gas phase MF are significantly reduced. About half of the MF has reacted to form $HCOO_{(a)}$ (~1370, ~1560 cm^{-1}) and $CH_3O_{(a)}$ (2827 cm^{-1}) as well as gas phase $CH_3OH_{(g)}$ (1032 cm^{-1}), $CO_{(g)}$ (2143 cm^{-1}), and $CO_{2(g)}$ (2349 cm^{-1}). After increasing the TiO_2 temperature to 400°C, the gas phase MF and $HCOO_{(a)}$ almost totally disappear. The signal of $CH_3O_{(a)}$ also largely reduces in intensity. Formation of $CH_2O_{(g)}$ and $CH_{4(g)}$ is identified by their characteristic absorptions at 1745 and 3017 cm^{-1}, respectively. $H_2O_{(g)}$ is present with characteristic bending absorptions between 1400 and 1650 cm^{-1}. Detailed relations between relative concentrations of gas products and TiO_2 surface temperatures are shown in Fig. 5. The concentration of MF in the gas phase decreases only slightly below ~200°C. Above this temperature, depletion of MF is accelerated, accompanying evolution of the gas products. As shown in Fig. 3, the TiO_2 surface is mainly adsorbed with $HCOO_{(a)}$ and $CH_3O_{(a)}$ at temperatures above 200°C, so the gas products from MF decomposition are expected to be due to the reactions of these adsorbed species with the TiO_2 surface. $HCOO_{(a)}$ is the key species for the formation of $CO_{(g)}$ and $CO_{2(g)}$. Their appearance temperature in this study is consistent with previous reports of $HCOO_{(a)}$ decomposition on TiO_2 (33–35). On the other hand, $CH_3O_{(a)}$ is the species initiating the reactions for the generation of $CH_2O_{(g)}$ and $CH_{4(g)}$ (31, 32, 36). It may dehydrogenate to generate $CH_2O_{(g)}$ and decompose very likely via methoxy C–O bond scission to produce $CH_{4(g)}$. Thermal reactions of MF over TiO_2 in the presence of O_2 were also studied. In the reactions of TiO_2 in contact with 2 Torr of MF and 5 Torr of O_2, no $CH_{4(g)}$ is found. As a contrast, the concentrations of $H_2O_{(g)}$, $CO_{(g)}$, $CO_{2(g)}$, and $CH_2O_{(g)}$ are 2–3 times those from the reaction in the

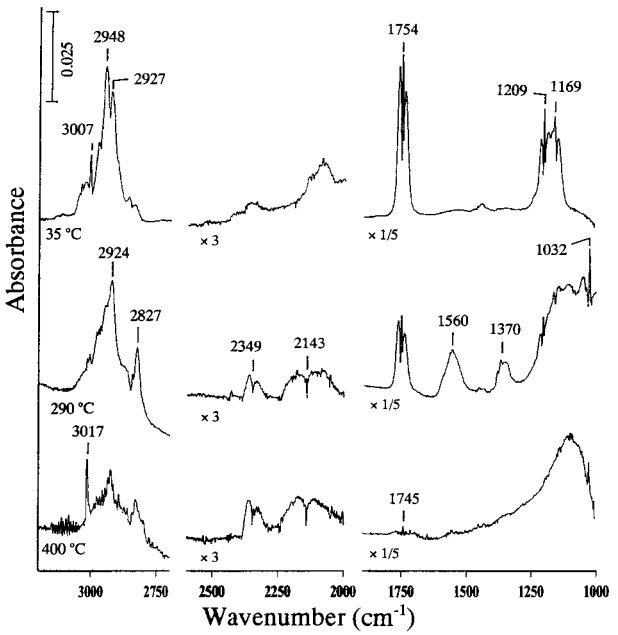

FIG. 4. Development of infrared spectra of 2 Torr of methyl formate over the TiO_2 surface heated at a rate of 2°C/s. All the spectra were recorded with 5 scans at the indicated temperatures. The TiO_2 powder used was 0.034 g.

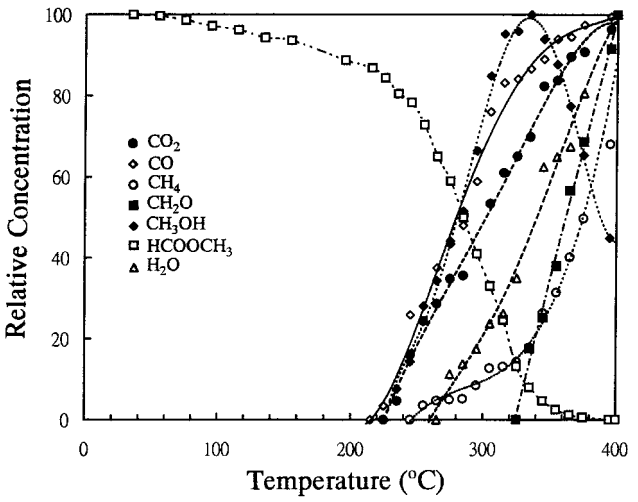

FIG. 5. Relative concentrations of the gas species involved in the thermal reactions of 2 Torr of methyl formate over TiO_2 as a function of surface temperature increased at a rate of 2°C/s. The maximum amount of each gas species during the heating process is scaled to 100%.

absence of oxygen. Previous studies (35, 36) have suggested that $CH_{4(g)}$ formation from decomposition of $CH_3O_{(a)}$ on TiO_2 is probably initiated by C–O bond scission to fill surface oxygen vacancies, forming CH_3 species. A portion of these methyl groups may dissociate to generate hydrogen on the surface at the reaction temperatures. The hydrogen rapidly reacts with remaining methyl groups to form $CH_{4(g)}$. It is not surprising that the $CH_{4(g)}$ formation channel is blocked as these vacancies are effectively filled in the presence of oxygen. Presumably, carbon atoms originally consumed in the desorption of $CH_{4(g)}$ are now used in the formation of the oxidized products of $CO_{(g)}$, $CO_{2(g)}$, and $CH_2O_{(g)}$ in the presence of O_2. Similarly, hydrogen atoms consumed in $CH_{4(g)}$ are now used in the formation of $H_2O_{(g)}$ and $CH_2O_{(g)}$. In $CH_3OH_{(g)}$ formation, similar concentrations are found both in the absence and presence of O_2, showing an insignificant effect of O_2 on its formation.

Adsorption of iodomethyl methyl ether. Figure 6 shows the IR spectra after IMME adsorption on TiO_2 followed by evacuation at the indicated temperatures. The gas phase IMME spectrum obtained by our IR spectrometer is also displayed for comparison. For the IR spectrum at 35°C, absorption bands at 1350, 1450, 1555, 1655, 2830, 2850, 2890, 2948, and 2995 cm^{-1} are observed. Among them, both 1350 and 1555 cm^{-1} are characteristic of $HCOO_{(a)}$. The absorption at 1655 cm^{-1} is generally assignable to carbonyl or carbon–carbon double-bond stretching vibration. The other bands are similar to the gas phase ones, implying that the CH_2OCH_3 moiety may hold its integrity on the TiO_2 surface at 35°C. After heating to 100°C, the three peaks of 1350, 1555, and 1655 cm^{-1} increase in intensity. Meanwhile, in the CH_x stretching region, new absorption features develop at 2830 and 2935 cm^{-1} that are attributable to $CH_3O_{(a)}$. At 150°C, the 1655 cm^{-1} band disappears and the distinct absorption bands of $CH_3O_{(a)}$ and $HCOO_{(a)}$ increase in intensity. After increasing the TiO_2 temperature to 200°C, IR absorption features similar to those of 150°C are observed. However, above 200°C, all the peaks decrease in intensity. Note, the surface heating in this study was performed under vacuum; therefore, any reaction products generated in the gas phase were unable to be detected. To investigate possible gas products, thermal reactions of TiO_2 in contact with 2 Torr of IMME were carried out by heating the surface from 35 to 350°C at a rate of 2°C/s. Three major gas products, $CH_2O_{(g)}$ (1745 cm^{-1}), $MF_{(g)}$ (1754 cm^{-1}), and $CH_{4(g)}$ (3017 cm^{-1}), are observed in this experiment. $CH_2O_{(g)}$ starts to evolve at ~110°C and monotonically increases to the end of the heating. $CH_{4(g)}$ appears at ~270°C and continues to increase to the end of the heating. MF becomes visible at ~110°C, reaches a maximum at ~250°C, and then declines. Since only carbonyl-containing products are observed in this study, the 1655 cm^{-1} peak present on the TiO_2 surface after the adsorption of IMME shown in Fig. 6 is more likely due to a carbonyl group instead of a carbon–carbon double bond. It may result from the formation of adsorbed CH_2O or MF interacting with the TiO_2 surface via the carbonyl group.

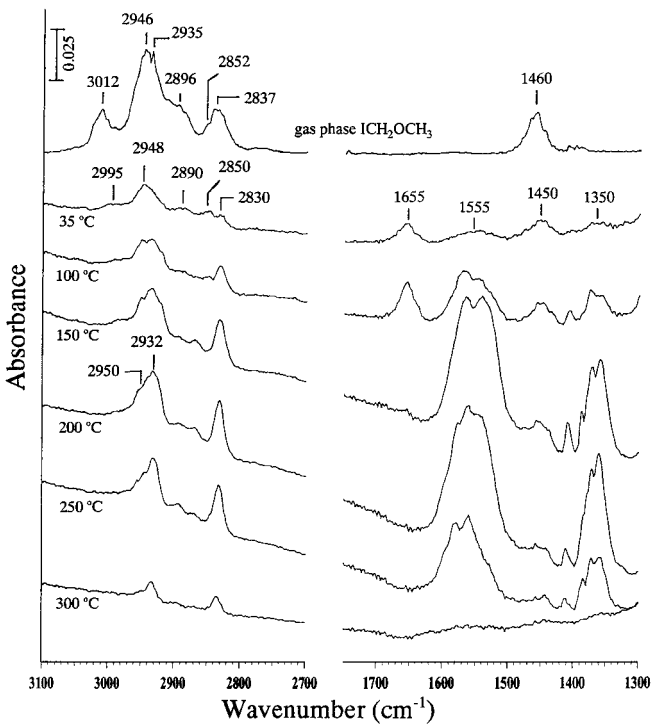

FIG. 6. Infrared spectra of the TiO_2 at 35°C after being in contact with 2 Torr of iodomethyl methyl ether followed by evacuation at the indicated temperatures for 1 min. All the spectra were obtained with 50 scans. The TiO_2 powder used was 0.05 g.

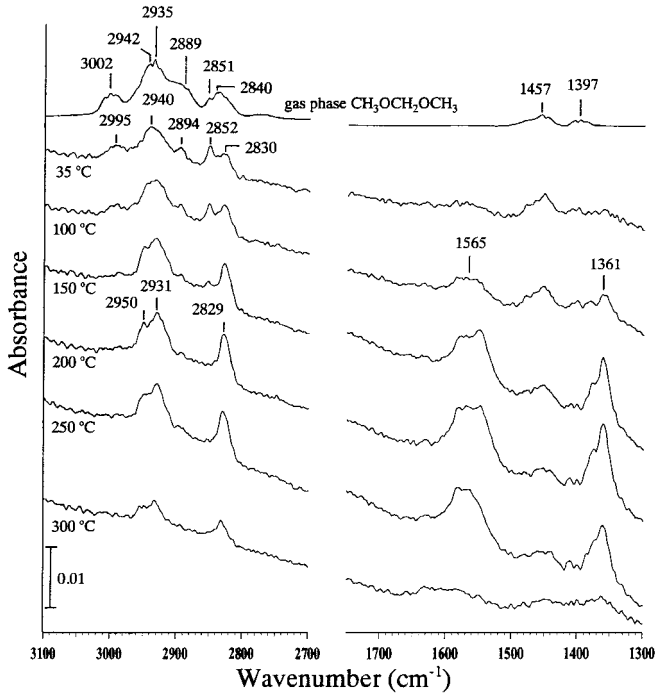

FIG. 7. Infrared spectra of the TiO_2 at 35°C after being in contact with 2 Torr of dimethoxymethane followed by evacuation at the indicated temperatures for 1 min. All the spectra were obtained with 50 scans. The TiO_2 powder used was 0.033 g.

Adsorption of dimethoxymethane. Figure 7 shows the IR spectra of DMM adsorption on TiO_2 followed by evacuation at the indicated temperatures. The gas phase DMM IR spectrum obtained by our spectrometer is also displayed for comparison. For the spectrum at 35°C, although the small characteristic absorptions at 1361 and 1565 cm^{-1} indicate that small amounts of DMM may already have dissociated on TiO_2, the absorption features in the CH_x stretching region are similar to the gas phase, suggesting that appreciable amounts of the adsorbed species are intact DMM. After heating to 150°C, the characteristic absorptions of $CH_3O_{(a)}$ become more clear in the CH_x stretch region. The surface amount of $HCOO_{(a)}$ also increases. Above 250°C, these species diminish.

Photochemistry of MF. Figure 8 shows the IR spectra of photocatalyzed MF oxidation over TiO_2 in the presence of oxygen at various UV irradiation times. Because the surface temperature raised to ~170°C upon UV irradiation, a thermal control experiment was carried out as well. In this experiment, the TiO_2 was exposed to 2 Torr of MF at 170°C and the IR spectrum was then monitored as a function of time while holding the TiO_2 sample at this temperature. This thermal effect on MF decomposition is shown in Fig. 8a and discussed first. The gas phase MF decreases in concentration with annealing time; its concentration for 1785 s reaches ~40% of the initial one. After such an annealing, surface absorptions at 2825 and 2865 cm^{-1} become more apparent, as can be observed in Fig. 3, which shows TiO_2 exposed to MF followed by evacuation at higher temperatures. $CO_{(g)}$ and $CO_{2(g)}$, growing with the annealing, appear at 2143 and 2349 cm^{-1}, respectively. $CH_2O_{(g)}$ absorptions become visible only after ~1600 s. In the case of UV irradiation as shown in Fig. 8b, in contrast to the thermal effect, a large portion of MF has already been destroyed after 500 s of irradiation, yielding a relatively large $CO_{2(g)}$ infrared absorption and well-resolved sharp peaks scattered in the CH_x stretching range. These peaks together with the concurrent absorption at 1745 cm^{-1} (not shown) indicate the formation of $CH_2O_{(g)}$. In addition, $H_2O_{(g)}$ signals are also observed. For the spectrum after 1785 s of irradiation, the gas phase MF and CH_2O almost disappear and the TiO_2 surface is left with $HCOO_{(a)}$ showing its characteristic peaks, similar to those shown in Fig. 1. Detailed relative concentrations of the gas species produced and MF as a function of UV irradiation time are shown in Fig. 9. MF gradually decreases with the UV irradiation and completely disappears after ~1000 s. $CH_2O_{(g)}$ signal appears at ~100 s, reaches its maximum at ~550 s, and then gradually decays. $CO_{(g)}$ appears after ~200 s and amounts to the maximum at ~1300 s over which it slowly decreases, presumably, by further oxidation to $CO_{2(g)}$. $CO_{2(g)}$ and $H_2O_{(g)}$, instead, monotonically increase with the UV irradiation. Another two control

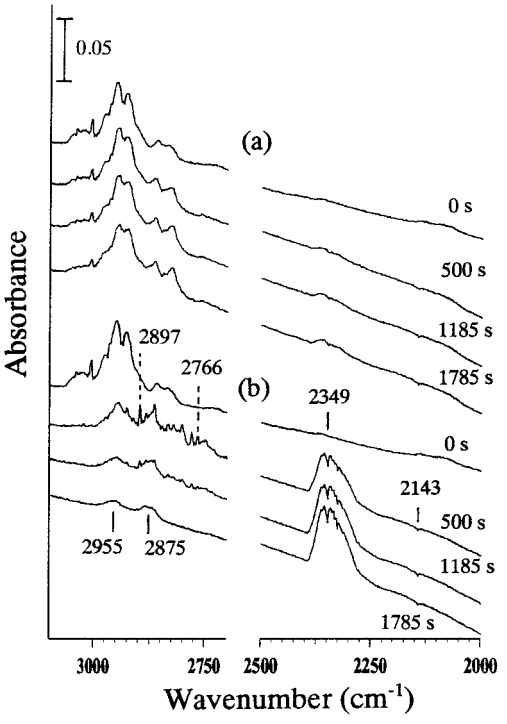

FIG. 8. Development of infrared spectra of a mixture of 2 Torr of methyl formate and 5 Torr of O_2 over the TiO_2 surface annealed at ~170°C (a) and irradiated with UV light (b) for the indicated time. The TiO_2 powder used was 0.036 g.

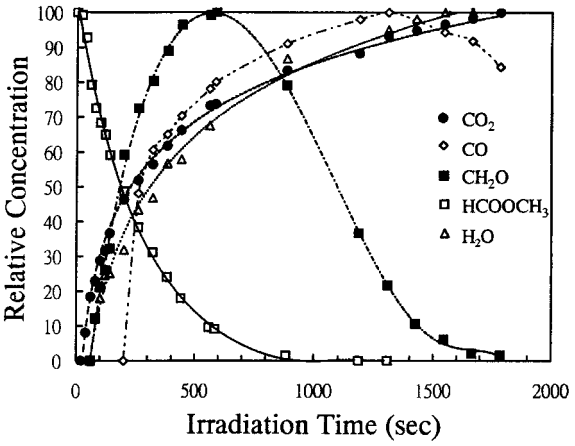

FIG. 9. Relative concentrations of the gas species involved in the photoreactions of a mixture of 2 Torr of methyl formate and 5 Torr of O_2 over TiO_2 as a function of UV irradiation time.

experiments were performed to check the roles of TiO_2 and O_2. The experiment using the same conditions as those used for the experiment in Fig. 8b, but without TiO_2, shows that the concentration of MF remains almost unchanged after 2000 s of UV irradiation, indicating that TiO_2 is essential to catalyze the MF decomposition. In the other control experiment in the absence of O_2, although $CO_{(g)}$, $CO_{2(g)}$, $CH_3OH_{(g)}$, and $CH_{4(g)}$ are observed, they are totally thermal products due to surface heating upon UV irradiation. Therefore, it is concluded that O_2 is also essential in the photooxidation of MF on TiO_2.

DISCUSSION

Adsorption and reactions of MF on several surfaces including Ag, Ni, Cu, SiO_2, Cu/SiO_2, and metal oxides have been studied. Table 1 compares the vibrational frequencies of MF on various surfaces. MF is reversibly adsorbed on Ag(111). At coverages below 1 ML (monolayer), as evidenced by the study of reflection absorption infrared spectroscopy, the molecular symmetry plane of the adsorbed MF lies perpendicular to the Ag(111) surface with the carbonyl axis tilted with respect to the surface and the methyl group pointed toward the surface. According to the red-shifted carbonyl vibration, which is also observed in the interaction of MF with Lewis acids, it is claimed that the carbonyl oxygen is pointed toward the Ag(111). Due to such an adsorption geometry, only vibrations with a' symmetry are observable (see Table 1) in terms of the dipole selection rule of surface vibrations, which states that only those vibrations with nonvanishing dynamic dipole moments normal to the surface are active. As the coverage increases to 5 ML, because the MF molecules in the multilayers may be adsorbed with its molecular plane tilted with respect to the surface, symmetry species other than a' can also contribute to the infrared absorption. On Ni(111), MF is molecularly adsorbed on the surface at −187°C with its orientation and coordination at submonolayer coverages similar to those when it is adsorbed on Ag(111). However, MF decomposes on Ni(111) surface at elevated temperatures mainly to form $CO_{(g)}$ and $H_{2(g)}$ as observed by temperature-programmed reaction/desorption investigation. On Cu(110), MF is also molecularly adsorbed at −133°C with a red-shifted carbonyl frequency as revealed by electron energy-loss spectroscopy. The adsorbed MF molecules almost completely desorb from the surface by −25°C with negligible reaction forming $CO_{2(g)}$, $CH_2O_{(g)}$, and $CH_3OH_{(g)}$ at temperatures higher than 25°C. On powdered SiO_2, MF molecules are adsorbed without decomposition at 27°C. Except for a slightly red-shifted carbonyl stretch, the infrared absorptions observed are similar to those in Ar matrix. In the cases of metal oxides, MF reacts with ZnO and ZnO(001), leading primarily to the formation of $H_{2(g)}$, $CO_{(g)}$, and $CO_{2(g)}$. Based on the similar kinetics and reaction pathways, it is suggested that the decomposition of MF on these surfaces is via $CH_3O_{(a)}$ and $HCOO_{(a)}$.

In the present TiO_2 study, MF is adsorbed molecularly at 35°C with absorption frequencies at 1675, 2960, and

TABLE 1

Comparison of Vibrational Frequencies (cm^{-1}) of Methyl Formate Adsorbed on Various Surfaces with Those on TiO_2 in the Present Study

MF/Ag(111) (0.7 ML, −153°C) (Ref. 3)	MF/Ag(111) (>5 ML, −153°C) (Ref. 3)	MF/Ni(111) (1 ML, −187°C) (Ref. 4)	MF/Cu(110) (1 ML, −133°C) (Ref. 5)	MF/SiO_2 (27°C) (Ref. 9)	MF Ar-matrix (Ref. 37)	MF liquid (Ref. 38)	MF vapor (Refs. 38–40)	Approx. description (Mode, symm. species) (Ref. 37)	MF/TiO_2 (35°C)
1677	1677	1659	1670						
1742	1703			1718	1746	1728	1754	C=O (ν_4, a')	1675
	1733								
				2850					
				2900					
				2952	2938			CH (ν_3, a')	
	2959	2985	2980	2964	2963	2957	2969	CH_3 (ν_2, a')	2960
	3015			3017	3014		3012	CH_3 (ν_{13}, a'')	
2984	2984	3042	3050	3044	3033			CH_3 (ν_1, a')	3040

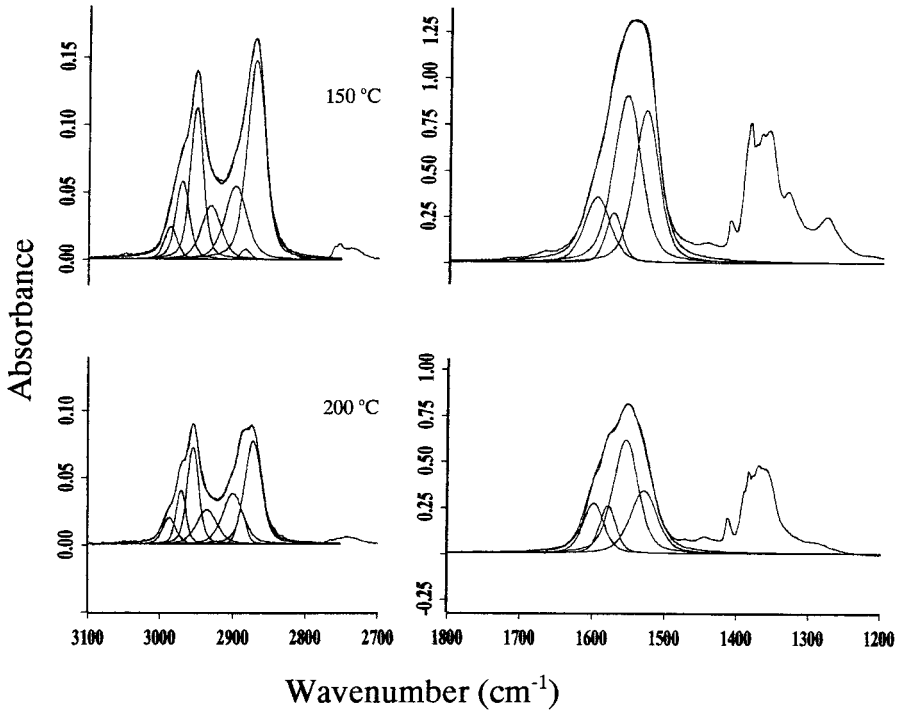

FIG. 10. Curve fitting for the IR spectra after formic acid adsorption followed by evacuation at 150 and 200°C. Each deconvoluted band is made of 40% Lorenz + 60% Gauss. The composed spectra for all of the deconvoluted bands are also shown.

3040 cm^{-1}. These absorption frequencies are also listed in the last column of Table 1 for comparison. The red-shifted carbonyl stretch is naturally attributable to the adsorbed MF molecules coordinating, via the carbonyl oxygen, to the Lewis sites on the TiO_2 surface. The adsorbed MF is almost completely removed from the surface by 150°C and the surface is mainly covered with adsorbed formate, methoxy, and an unidentified species with frequencies of 2866 and 2943 cm^{-1}. Considering the surface site heterogeniety, possible different bonding structures of adsorbed species, and coexistence of several adsorbed species on the TiO_2 surface, curve fitting procedures for the spectra after the adsorption of formic acid, methanol, and MF followed by evacuation at 150 and 200°C were carried out for more detailed IR data interpretation. All of the characteristics of the deconvoluted bands obtained in the curve fitting, including band position, width, and area, are listed in the Appendix. Figure 10 shows the same spectra as shown in Fig. 1 at 150 and 200°C as well as the deconvoluted bands and their composed spectra. The total band area in the region of 1450–1750 cm^{-1} is ~8.2 times that in the region of 2800–3050 cm^{-1}. Figure 11 presents the same spectra as shown in Fig. 2 at 150 and 200°C as well as the deconvoluted bands and their composed spectra. Figure 12 shows the same spectra as shown in Fig. 3 at 150 and 200°C as well as the deconvoluted bands and their composed spectra. Since methoxy and formate groups are present on the surface after the adsorption of MF followed by evacuation at 150 and 200°C,

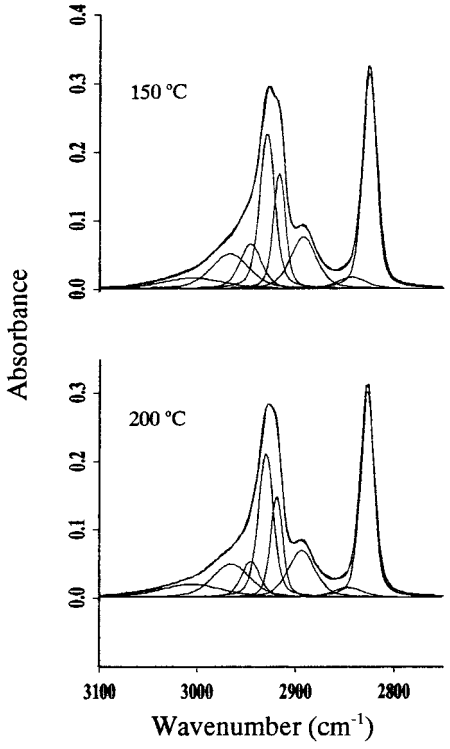

FIG. 11. Curve fitting for the IR spectra after methanol adsorption followed by evacuation at 150 and 200°C. Each deconvoluted band is made of 40% Lorenz + 60% Gauss. The composed spectra for all of the deconvoluted bands are also shown.

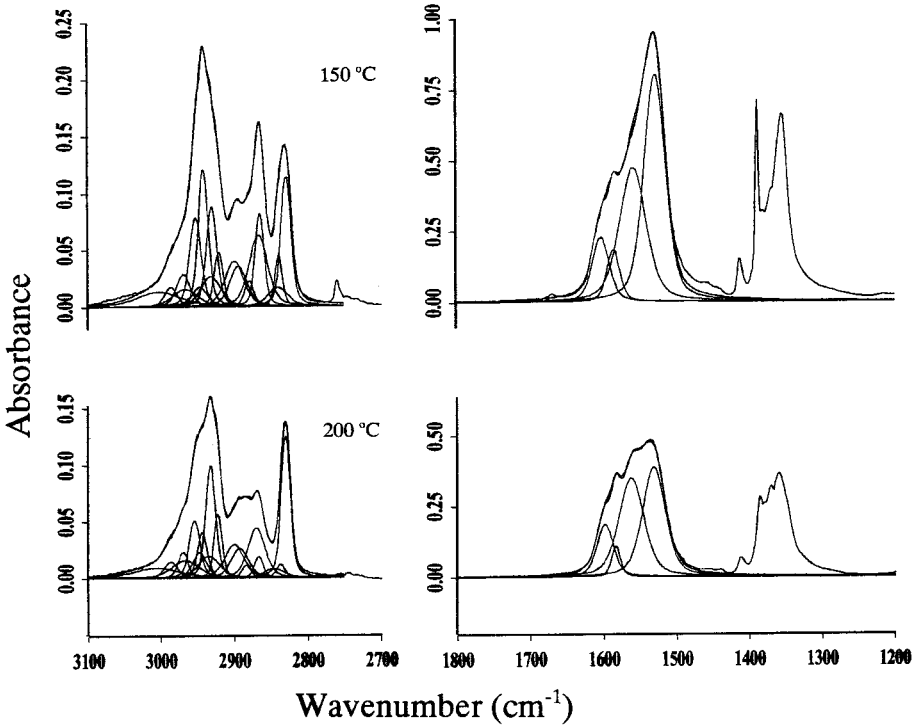

FIG. 12. Curve fitting for the IR spectra after methyl formate adsorption followed by evacuation at 150 and 200°C. Each deconvoluted band is made of 40% Lorenz + 60% Gauss. The composed spectra for all of the deconvoluted bands are also shown.

the deconvoluted bands in Figs. 10 and 11 were also used in fitting MF spectra at the corresponding temperatures, but allowing variations in peak position, width, and area for optimizing the curve fit. Furthermore, since the total band area in the region of 1450–1750 cm^{-1} is ~8.2 times that in the region of 2800–3050 cm^{-1} in Fig. 10, the total band area in the 2800–3050 cm^{-1} region from formate contribution is limited to ~1/8.2 that in the 1450–1750 cm^{-1} region in the case of fitting MF spectra. It is found that in addition to the contribution of methoxy and formate groups, three bands at 2841, 2866, and 2942 cm^{-1} are needed to obtain an optimized fit. To further identify the adsorbed species responsible for these three peaks, adsorption and reactions of IMME and DMM on TiO_2 have been studied, because they are possible precursor molecules for generating adsorbed hemiacetal alcoholate ($-OCH_2OCH_3$) groups, which are thought to be the reaction intermediate for MF decomposition on copper-based catalysts (18). The vibrational frequencies of IMME adsorbed on TiO_2 at 35°C are listed in the first column in Table 2. Although the

TABLE 2

Comparison of Vibrational Frequencies (cm^{-1}) of Iodomethyl Methyl Ether, Dimethoxymethane, 1,1,1-Trimethoxyethane, and Methyl Formate

Iodomethyl methyl ether/TiO_2 (35°C)	Approx. description (Ref. 41)	Dimethoxy-methane/TiO_2 (35°C)	Approx. description (Refs. 43, 44)	1,1,1-Trimethoxy ethane Vapor (Ref. 45)	1,1,1-Trimethoxy ethane Liquid (Ref. 45)	Approx. description (Ref. 45)	MF/TiO_2 (150°C)
1655							
2830	ν_3 CH_3	2830	ν CH_3				
2848	ν_2 CH_2, ν_2 CH_3	2852	ν CH_2, ν CH_3	2846	2833	ν_4, ν_{44} OCH_3	2841
2890	2δ CH_2, 2δ CH_3	2894	2δ CH_2, 2δ CH_3				2866
2948		2940		2923	2915	ν_3 CCH_3	
2995	ν_1 CH_3, ν_1 CH_2	2995	ν CH_2, ν CH_3	2958	2946	ν_1, ν_2, ν_{20}	2942
				2965		ν_{21} OCH_3	
				2975			
				3002	2998	ν_{19} CCH_3	

appearance of the peak at 1655 cm^{-1} is likely due to adsorbed MF or CH_2O from decomposition of IMME on TiO_2, the absorption features in the CH_x stretching region are similar to those of IMME in the gas phase. This resemblance implies that most of the IMME molecules after adsorption may remain intact on TiO_2 at 35°C. But it is worth noting the recent study of adsorption of methyl iodide on TiO_2 in which it was found that the C–I bond in methyl iodide breaks on TiO_2 at 35°C to form $CH_3O_{(a)}$ (42). If this also occurs for IMME on TiO_2, OCH_2OCH_3 groups are expected to be present on the surface. It may show absorption features in the CH_x region similar to those of IMME in the gas phase. In either case, some of these adsorbed species have reacted on the TiO_2 surface at 150°C to increase the amount of methoxy and formate groups. In DMM, the CH_x stretching absorptions after adsorption at 35°C, also included in Table 2, resemble those in the gas phase, indicating that most of the DMM molecules are adsorbed as a whole. These absorption features change after heating the TiO_2 to 150°C due to the formation of methoxy and formate groups. In both IMME and DMM, no peak at ~2866 cm^{-1} with intensity comparable to that of the peak at ~2830 cm^{-1} in methoxy is found, strongly suggesting that MF decomposition on TiO_2 is unlikely via the $-OCH_2OCH_3$ intermediate. An orthoester-type species, similar to the one proposed after MF adsorption on oxygen preadsorbed Ag(110), is proposed to be the intermediate on TiO_2 (see Scheme 3).

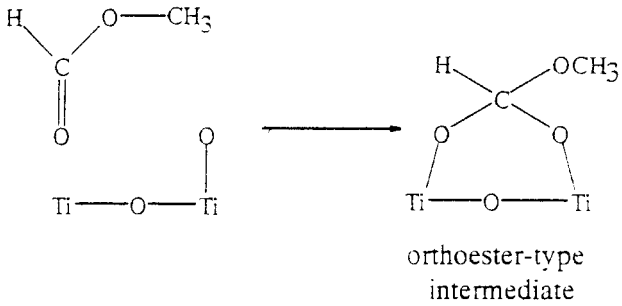

SCHEME 3

The CH_x stretching frequencies of 1,1,1-trimethoxy ethane, which also contains an orthoester backbone, are included in Table 2. By comparing these frequencies with 2841, 2866, and 2942 cm^{-1} bands belonging to the proposed orthoester-type intermediate, the 2841 and 2942 cm^{-1} bands are assigned to symmetric and antisymmetric -OCH_3 stretches, respectively. The 2866 cm^{-1} band may be assigned to the CH stretch or to overtone of CH_3 deformation. MF adsorption on TiO_2 can be described by MF chemically bonded at an acid–base site pair consisting of an acidic titanium cation and a basic oxygen anion. MF is first coordinated at the Lewis acid sites via the oxygen atom of the carbonyl group. The carbon of the carbonyl becomes more electrophilic due to this coordination and is subject to an attack from a neighboring nucleophilic surface oxygen anion. A similar adsorption geometry has been discussed previously in the study of CH_2O adsorbed on TiO_2 to form dioxymethylene surface species (46).

In photochemistry of MF over TiO_2, appreciable reactions only proceed in the presence of oxygen to form $CO_{(g)}$, $CO_{2(g)}$, $CH_2O_{(g)}$, and $H_2O_{(g)}$. Note that CH_2O gas molecules are photosensitive for the UV wavelength used in this study and may produce $CO_{(g)}$ by photodecomposition (47). Adsorption and thermal reactions of CH_2O on TiO_2 have been studied previously (26, 46). Its reactions are initiated by a dioxymethylene intermediate which is formed as CH_2O is adsorbed at a cation–anion site pair on the surface. On fully oxidized TiO_2 surfaces, dioxymethylene undergoes Cannizzaro-type disproportionation by hydride transfer to yield $CH_3O_{(a)}$ and $HCOO_{(a)}$. On the other hand, on reduced TiO_2 surfaces, dioxymethylene may be directly reduced to $CH_3O_{(a)}$ and be totally decomposed to $C_{(a)}$, $H_{(a)}$, and $O_{(a)}$. Since in the present photostudy the TiO_2 surface is mainly covered with the orthoester-type species, $CH_3O_{(a)}$, and $HCOO_{(a)}$ for the experimental conditions used, these adsorbed species must play important roles in governing the reaction kinetics. It is known that when TiO_2 or ZnO in formic solutions is irradiated with UV light $CO_{2(g)}$ is formed (48–50). A two-step mechanism has been previously proposed to explain formate oxidation on a ZnO single-crystal electrode (50). In that mechanism formate oxidation is initiated by receiving photogenerated holes to produce formyloxy radicals ($HCOO^{\bullet}$), which then inject electrons into the ZnO conduction band to form $CO_{2(g)}$. Photochemistry of $CH_3O_{(a)}$ on TiO_2 has been recently investigated by *in situ* mass spectrometry and infrared spectroscopy (51). In the absence of oxygen, the $CH_3O_{(a)}$ is oxidized to $CH_2O_{(g)}$. A mechanism supported by electron paramagnetic study has been proposed. $CH_3O_{(a)}$ receives photoholes upon UV irradiation to form $-OCH_2^{\bullet}$ radicals, which then further decompose to generate $CH_2O_{(g)}$. This photoprocess is severely retarded for prolonged irradiation, because the photoelectrons may accumulate on the surface, thus increasing the rate of electron–hole recombination so as to reduce the photoefficiency. Another photoreaction pathway steps in as oxygen is added in the reaction system, resulting in the formation of $H_2O_{(a)}$ and $HCOO_{(a)}$. In the presence of oxygen, the photoreaction of $CH_3O_{(a)}$ may be likely via the so-called "Russell-like mechanism" (52). Oxygen plays two roles in this mechanism: it may recombine with $-OCH_2^{\bullet}$ radicals to form $-OCH_2OO^{\bullet}$ as well as receive photoelectrons and recombine with H^+ to yield $HOO^{\bullet}$. H^+ is formed from the photodecomposition of $CH_3O_{(a)}$ after receiving the photoholes. $-OCH_2OO^{\bullet}$ and $HOO^{\bullet}$ can recombine to generate $-OCH_2OOOOH$ tetraoxide, which decomposes to yield $H_2O_{(a)}$ and $HCOO_{(a)}$. At last, as to the photochemistry of the adsorbed orthoester-type intermediate, no detailed pathways can be determined from the present study.

In the photochemical process involving aqueous suspensions of TiO_2 or in powdered TiO_2, O_2^{-1}, O_2^{-2}, O_3^{-1}, and O_3^{-3} have been detected (53–63). In addition to the possibility of holes, some of them may actually participate as oxidants in the photoreaction of the orthoester-type intermediate.

CONCLUSIONS

The temperature-dependent adsorption of MF on powdered TiO_2 has been investigated using infrared spectroscopy. This study reveals the thermal decomposition process of MF and its reaction kinetics. When MF is adsorbed on an acid–base site pair on TiO_2, it reorganizes on the surface, losing the carbonyl characteristics and forming an orthoester-type intermediate. Another possible adsorbed hemiacetal intermediate in the decomposition of methyl formate, which is thought to be important on copper-based catalysts, has been ruled out using two model compounds of iodomethyl methyl ether and dimethoxymethane. In MF photochemistry in this study, appreciable photoreactions proceed only in the presence of both TiO_2 catalyst and O_2.

APPENDIX

The data in parentheses are the band position, width, and area, respectively, for each deconvoluted band.

For fitting the IR spectra after formic acid adsorption followed by evacuation at 150°C: (1530.6, 39.77, 41.49), (1557.4, 44.64, 51.06), (1575.3, 25.97, 8.88), (1598.1, 41.4, 18.6), (2885.5, 15.41, 0.15), (2899.2, 35.12, 2.42), (2932.5, 31.18, 1.58), (2952.7, 20.07, 2.87), (2971.7, 21.14, 1.54), (2987.5, 20.43, 0.62).

For fitting the IR spectra after formic acid adsorption followed by evacuation at 200°C: (1529.8, 43.8, 18.9), (1555, 40.6, 31.6), (1579.4, 25.98, 8.55), (1598.9, 33.28, 11.57), (2873.3, 26.88, 2.62), (2889.1, 14.33, 0.453), (2900.9, 32.97, 1.58), (2936.5, 32.25, 1.05), (2955.2, 17.92, 1.65), (2971.3, 15.41, 0.786), (2987.5, 21.14, 0.53).

For fitting the IR spectra after methanol adsorption followed by evacuation at 150°C: (2826.4, 15.93, 6.39), (2844.5, 33.98, 0.72), (2893.5, 30.8, 2.94), (2917.9, 14.16, 3.02), (2947, 25.13, 2.08), (2967.9, 44.25, 2.85), (3005.8, 73.63, 1.46).

For fitting the IR spectra after methanol adsorption followed by evacuation at 200°C: (2828.2, 15.58, 6), (2847.7, 35.4, 0.64), (2894.5, 31.86, 2.78), (2920.1, 14.16, 2.65), (2931.1, 17.7, 4.72), (2946.3, 21.59, 1.44), (2966.2, 43.9, 2.73), (3006.6, 73.99, 1.79).

For fitting the IR spectra after methyl formate adsorption followed by evacuation at 150°C: (2830, 15.58, 2.26), (2840.3, 11.33, 0.65), (2841.3, 31.15, 0.66), (2865.8, 13.45, 1.4), (2867.6, 28.67, 2.27), (2880, 14.16, 0.4), (2894.9, 27.26, 1.23), (2900.2, 29.73, 1.5), (2921.5, 13.45, 0.81), (2930.7, 15.93, 1.79), (2932.1, 31.15, 1.04), (2942.1, 15.22, 2.34), (2947, 23.01, 0.5), (2952.7, 18.05, 1.8), (2966.9, 40.71, 0.78), (2969.4, 22.30, 0.8), (2986.4, 19.82, 0.43), (3003, 72.57, 1.2).

For fitting the IR spectra after methyl formate adsorption followed by evacuation at 200°C: (2831.3, 14.33, 2.27), (2838.5, 12.9, 0.2), (2847.1, 32.61, 0.33), (2867.9, 13.26, 0.32), (2871.2, 26.88, 1.5), (2884.8, 13.62, 0.19), (2893.8, 27.24, 0.9), (2901, 30.46, 1.14), (2923.2, 11.83, 0.85), (2932.9, 15.05, 1.9), (2935.4, 33.69, 0.82), (2944.4, 15.05, 0.76), (2948, 21.5, 0.62), (2954.8, 16.84, 1.08), (2967.4, 44.08, 0.86), (2970.7, 15.77, 0.45), (2987.2, 20.79, 0.38), (3006.5, 74.9, 0.86).

ACKNOWLEDGMENT

We gratefully acknowledge the financial support of the National Science Council of the Republic of China (Grant NSC-87-2113-M-006-014) for this research.

REFERENCES

1. Lee, J. S., Kim, J. C., and Kim, Y. G., *Appl. Catal.* **57**, 1 (1990).
2. Wachs, I. E., and Madix, R. A., *Surf. Sci.* **76**, 531 (1978).
3. Schwaner, A. L., Fieberg, J. E., and White, J. M., *J. Phys. Chem. B* **101**, 11-112 (1997).
4. Zahidi, E., Castonguay, M., and Mcbreen, P., *J. Am. Chem. Soc.* **116**, 5847 (1994).
5. Sexton, B. A., Hughes, A. E., and Avery, N. R., *Surf. Sci.* **155**, 366 (1985).
6. Bowker, M., Houghton, H., and Waugh, K. C., *J. Chem. Soc. Faraday Trans. 1* **78**, 2573 (1982).
7. Vohs, J. M., and Barteau, M. A., *Surf. Sci.* **197**, 109 (1988).
8. Peng, X. D., and Barteau, M. A., *Surf. Sci.* **224**, 327 (1989).
9. Millar, G. J., Rochester, C. H., and Waugh, K. C., *J. Chem. Soc. Faraday Trans.* **87**, 2785 (1991).
10. Millar, G. J., Rochester, C. H., and Waugh, K. C., *J. Catal.* **142**, 263 (1993).
11. Millar, G. J., Rochester, C. H., and Waugh, K. C., *J. Chem. Soc. Faraday Trans.* **88**, 3497 (1992).
12. Monti, D. M., Cant, N. M., Trimm, D. L., and Wainwright, M. S., *J. Catal.* **100**, 17 (1986).
13. Monti, D. M., Cant, N. M., Trimm, D. L., and Wainwright, M. S., *J. Catal.* **100**, 28 (1986).
14. Barteau, M. A., Bowker, M., and Madix, R. J., *Surf. Sci.* **94**, 303 (1980).
15. Nunan, J. G., Bogdan, C. E., Klier, K., Smith, K. J., Young, C.-W., and Herman, R. G., *J. Catal.* **113**, 410 (1988).
16. Takahashi, K., Takezawa, N., and Kobayashi, H., *Chem. Lett.* **7**, 1061 (1983).
17. Denise, B., and Seneden, R. P. A., *C1 Mol. Chem.* **1**, 307 (1985).
18. Sorum, P. A., and Onsager, O. T., *in* "Proceedings, 8th International Congress on Catalysis, Berlin, 1984," Vol. II, p. 233. Dechema, Frankfurt-am-Main, 1984.
19. Fox, M. A., and Dulay, M. A., *Chem. Rev.* **93**, 341 (1993).
20. Hoffmann, M. R., Martin, S. T., Choi, W., and Bahnemann, D. W., *Chem. Rev.* **95**, 69 (1995).
21. Liu, Y. C., Griffin, G. L., Chan, S. S., and Wachs, I. E., *J. Catal.* **94**, 108 (1985).
22. Carlson, T., and Griffin, G. L., *J. Phys. Chem.* **90**, 5896 (1986).
23. Basu, P., Ballinger, T. H., and Yates, J. T., Jr., *Rev. Sci. Instrum.* **59**, 1321 (1988).
24. Wong, J. C. S., Linsebigler, A., Lu, G., Fan, J., and Yates, J. T., Jr., *J. Phys. Chem.* **99**, 335 (1995).

25. Degussa Technical Bulletin Pigments, No. 56, p. 13, 1990.
26. Herzberg, Z., "Molecular Spectra and Molecular Structure II: Infrared and Raman Spectra of Polyatomic Molecules," Van Nostrand, New York, 1945.
27. Groff, R. P., and Manogue, M. H., *J. Catal.* **79**, 462 (1983).
28. Busca, G., Lamotte, J., Lavalley, J.-C., and Lorenzelli, V., *J. Am. Chem. Soc.* **109**, 5197 (1987).
29. Nakamoto, K., "Infrared and Raman Spectra of Inorganic and Coordination Compounds," 4th ed., pp. 232–233. Wiley & Sons, New York, 1986.
30. Suda, Y., Morimoto, T., and Nagao, M., *Langmuir* **3**, 99 (1988).
31. Taylor, E. A., and Griffin, G. L., *J. Phys. Chem.* **92**, 477 (1988).
32. Hussein, G. A. M., Sheppard, N., Zaki, M., and Fahim, R. B., *J. Chem. Soc. Faraday Trans.* **87**, 2655 (1991).
33. Onish, H., Aruga, T., and Iwasawa, Y., *J. Catal.* **146**, 557 (1994).
34. Kim, K. S., and Barteau, M. A., *Langmuir* **6**, 1485 (1990).
35. Kim, K. S., and Barteau, M. A., *Langmuir* **4**, 945 (1988).
36. Lusvardi, V. S., Barteau, M. A., and Farneth, W. E., *J. Catal.* **153**, 41 (1995).
37. Muller, R. P., Hollenstein, H., and Huber, J. R., *J. Mol. Struct.* **100**, 95 (1983).
38. Wilmhurst, J. K., *J. Mol. Struct.* **1**, 201 (1957).
39. Susi, H., and Scherer, J. R., *Spectrochim. Acta* **25A**, 1243 (1969).
40. Susi, H., and Zell, H., *Spectrochim. Acta* **19**, 1933 (1963).
41. McKean, D. C., Torto, I., and Morrisson, A. R., *J. Mol. Struct.* **99**, 101 (1983).
42. Su, C. S., Lin, J. C., Yeh, J. C., and Lin, J.-L., submitted to *J. Phys. Chem.*
43. Wladislaw, B., Giora, A., and Vicentini, G., *J. Chem. Soc. B* 586 (1966).
44. Nukada, K., *Spectrochim. Acta* **18**, 745 (1962).
45. Kumar, K., *J. Mol. Struct.* **12**, 19 (1972).
46. Idriss, H., Kim, K. S., and Barteau, M. A., *Surf. Sci.* **262**, 113 (1992).
47. Okabe, H., "Photochemistry of Small Molecules," Wiley & Sons, New York, 1978.
48. Bideau, M., Claudel, B., Faure, L., and Rachimoellah, M., *Chem. Eng. Commun.* **93**, 167 (1990).
49. Carraway, E. R., Hoffman, A. J., and Hoffmann, M. R., *Environ. Sci. Technol.* **28**, 786 (1994).
50. Morrison, S. R., and Freund, T., *J. Chem. Phys.* **47**, 1543 (1967).
51. Chuang, C.-C., Chen, C.-C., and Lin, J.-L., *J. Phys. Chem. B* **103**, 2439 (1999).
52. Schwitzgebel, J., Ekerdt, J. G., Gerischer, H., and Heller, A., *J. Phys. Chem.* **99**, 5633 (1995).
53. Meriaudeau, P., and Vedrine, A. C., *J. Chem. Soc. Faraday Trans. 2* **72**, 472 (1976).
54. Bickley, R. I., and Stone, F. S., *J. Catal.* **31**, 389 (1973).
55. Bickley, R. I., Munuera, G., and Stone, F. S., *J. Catal.* **31**, 398 (1973).
56. Munuera, G., Rives-Arnau, V., and Saucedo, A., *J. Chem. Soc. Faraday Trans. 1* **75**, 736 (1979).
57. Gonzalez-Elipe, A., Munuera, G., and Soria, J., *J. Chem. Soc. Faraday Trans. 1* **75**, 749 (1979).
58. Anpo, M., Aikawa, N., Kubokawa, Y., Che, M., Louis, C., and Giamello, E., *J. Phys. Chem.* **89**, 5017 (1985).
59. Anpo, M., Aikawa, N., Kubokawa, Y., Che, M., Louis, C., and Giamello, E., *J. Phys. Chem.* **89**, 5689 (1985).
60. Anpo, M., Kubokawa, Y., Fujii, T., and Suzuki, S., *J. Phys. Chem.* **88**, 2572 (1984).
61. Howe, R. F., and Grätzel, M., *J. Phys. Chem.* **91**, 3906 (1987).
62. Courbon, H., Formenti, M., and Pichat, P., *J. Phys. Chem.* **81**, 550 (1977).
63. Jaeger, C. D., and Bard, A. J., *J. Phys. Chem.* **83**, 3146 (1979).